Keynote Paper

Optimization of Organic NLO Materials for Integration with Silicon Photonic, Plasmonic (Metal Optics), and Metamaterial Devices

Larry R. Dalton*[a], Alex K.-Y. Jen[b], Bruce H. Robinson[a], Rene Overney[c], Stephanie J. Benight[a], Daniel B. Knorr, Jr.[c], Seongku Kim[d], Harold R. Fetterman[d], Cheng Zhang[e]
[a]Department of Chemistry, University of Washington, Seattle, WA 98195-1700; [b]Department of Material Science & Engineering, University of Washington, Seattle, WA 98195-2120; [c]Department of Chemical Engineering, University of Washington, Seattle, WA 98195-1750; [d]Department of Electrical Engineering, University of California at Los Angeles, Los Angeles, CA 90095; Department of Chemistry, Norfolk State University, Norfolk, VA 23504

ABSTRACT

Specific spatially-anisotropic interactions are identified that enhance noncentrosymmetric order required for electro-optic activity. Enhancement of electric-field-poling-induced noncentrosymmetric order by these specific interactions is shown to result from a reduction of lattice dimensionality from three to two dimensions. New analytical techniques for measurement of centrosymmetric and noncentrosymmetric order and lattice dimensionality are introduced. Measurement of order parameters is correlated with viscoelastic data to gain further insight into the influence of specific interactions on poling efficiency and thus material electro-optic activity. The integration of organic electro-optic materials into silicon photonic, plasmonic, and metamaterial devices is also discussed. These device structures can affect the "effective" optical nonlinearity of organic materials but care must be exercised to control optical loss.

Keywords: Organic electro-optic materials, plasmonics, silicon photonics, metamaterials, nano-engineering, intermolecular electrostatic interactions, Monte Carlo/molecular dynamics simulations

1. INTRODUCTION

Organic electro-optic (OEO) materials are well known to exhibit a number of important characteristics including ultrafast (femtosecond) response to time-dependent electric fields[1-5] and exceptional processability including the ability to be effectively integrated with diverse materials such as silicon photonics[5-13] and metal optics (plasmonics)[14]. It is also well-understood that OEO materials have the potential for very large electro-optic (EO) activity. The major problem in realizing exceptional EO activity relates to the difficulty of achieving high noncentrosymmetric (acentric) order in translating the exceptional first hyperpolarizability (β) of dipolar molecules (chromophores) to macroscopic material EO activity. For prolate-ellipsoid-shaped dipolar molecules, intermolecular dipolar interactions dramatically attenuate acentric order resulting in EO activity going through a maximum with chromophore number density and limiting electro-optic activity to a few percent of that possible for perfect order.[15,16] Some improvement in acentric order and thus EO activity can be realized by making chromophores more spherical in shape.[17] Incorporation of chromophores into multi-chromophore-containing dendrimers, where covalent bond potentials inhibit centrosymmetric pairing of chromophores, can also lead to improved EO activity.[18-21] More recently, certain specific spatially-anisotropic interactions have been shown to lead to an enhancement of electric field poling-induced noncentrosymmetric order.[22-30] Arene-perfluoroarene and coumarin-coumarin interactions have been shown to lead to factors of 2-3 enhancement of acentric order and to electro-optic activity in the range 150-450 pm/V.[22-26] Laser-assisted poling of host lattice materials also has been shown to lead to improvement in the acentric order of guest chromophores.[30] This general phenomenon has been referred to as matrix-assisted poling (MAP).[30] The MAP phenomenon has recently been shown to relate to lattice dimensionality.[24-26] Lattice dimensionality of electrically-poled OEO materials can, in turn, be defined by the ratio $\langle\cos^2\theta\rangle/\langle\cos^3\theta\rangle$ where $\langle\cos^2\theta\rangle$ is the centrosymmetric (centric) order parameter and $\langle\cos^3\theta\rangle$ is the noncentrosymmetric (acentric) order parameter.[26] These order parameters can be simulated by coarse-grained (pseudo-atomistic) Monte Carlo and molecular dynamics calculations.[20,21,31,] They can also be defined by measurement techniques such as variable angle polarization-referenced absorption spectroscopy (VAPRAS), variable angle spectroscopic ellipsometry (VASE), and attenuated total reflection (ATR).[20,21,26,32] ATR permits measurement of both elements (r_{33} and r_{13}) of the EO tensor for electrically-

Organic Photonic Materials and Devices XIII, edited by Robert L. Nelson, François Kajzar, Toshikuni Kaino, Yasuhiro Koike,
Proc. of SPIE Vol. 7935, 793502 · © 2011 SPIE · CCC code: 0277-786X/11/$18 · doi: 10.1117/12.881264

poled OEO materials. If the anisotropy of the molecular hyperpolarizability tensor (β) is measured or can be estimated from theory (semi-empirical or time-dependent density functional theory calculations), then $<\cos^3\theta>$ can be determined from the ratio r_{33}/r_{13}. The acentric order parameter can also be determined from the principal element r_{33} providing that β_{zzz} is determined from Hyper-Rayleigh Scattering (HRS) but again theory is required to relate β_{HRS} to β_{zzz}. Knowledge of dielectric permittivity and index of refraction is also required to determine $<\cos^3\theta>$ from r_{33}. Thus, measurement of $<\cos^3\theta>$ is an indirect characterization. Determination of $<\cos^2\theta>$ by VAPRAS and VASE, on the other hand, is a direct measurement. More quantitative definition of lattice dimensionality is achieved by numerical calculations[26] but lattice dimensionality (M) can be approximately related to the order parameters by the following relationship: $\left\langle \cos^3\theta \right\rangle \approx \sqrt{\left(\frac{9-2M}{2+M}\right)\left(\left\langle P_2 \right\rangle - \frac{3-M}{2M}\right)}$ where $\left\langle P_2 \right\rangle = \frac{3\left\langle \cos^2\theta \right\rangle - 1}{2}$.[26] We have examined a number of OEO materials (see Figs. 1-3). When MAP interactions are present, lattice dimensionality is reduced while for materials without such interactions, the experimentally-defined lattice dimensionality is approximately 3-D (see Table 1).[26]

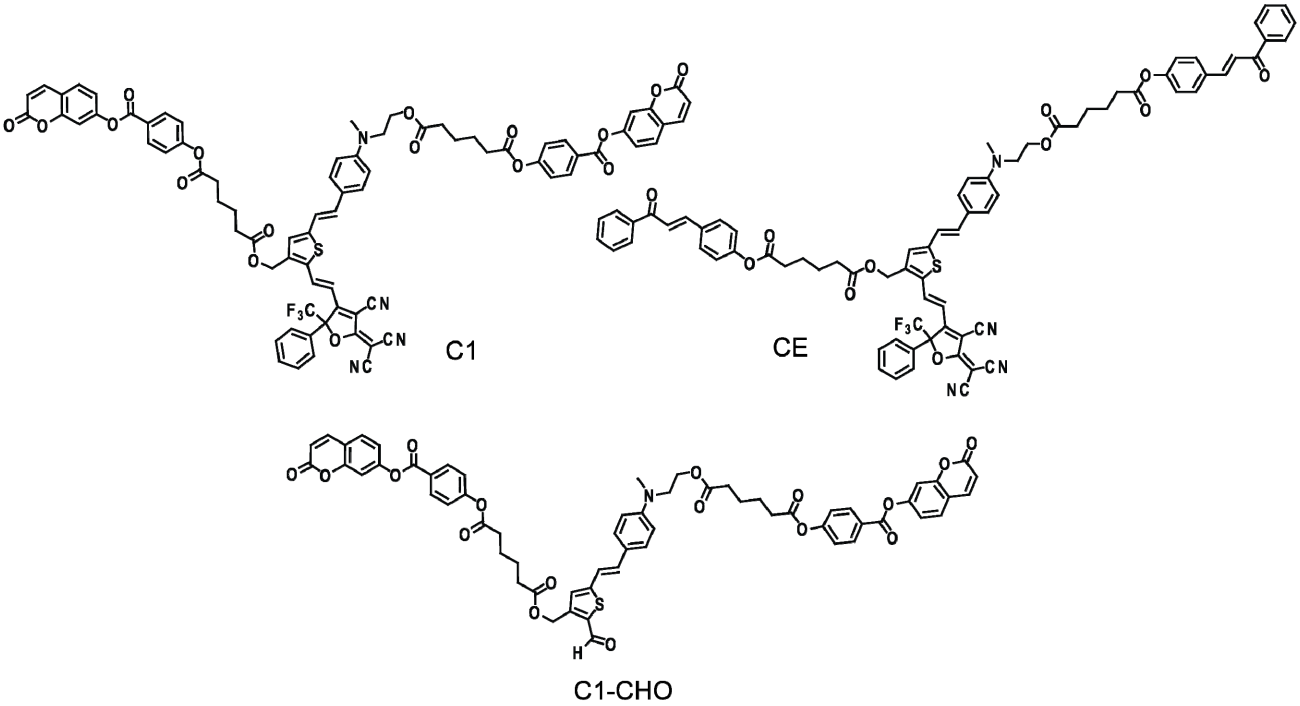

Figure 1. Structures of C1 and related EO chromophore-containing dendrimers.

Table 1. Order Parameter and Lattice Dimensionality Data for C1 and the FTC Chromophore in PMMA

Material	N	$<\cos^3\theta>$	$<P_2>$	M
C1	4.4×10^{20}/cc	0.15	0.19	2.2
FTC/PMMA*	3.6×10^{20}/cc	0.015	0.042	2.8

*FTC denotes the fundamental chromophore of the C1 dendrimer so the data in this table reflect the effect of different environments surrounding the FTC chromophore.

Evidence of the effect of MAP interactions on molecular order and cooperativity is also provided by nanoscopic viscoelastic measurements such as shear modulation force microscopy (SM-FM), intrinsic friction analysis (IFA), and dielectric relaxation spectroscopy (DRS).[33-38] If MAP interactions are absent, the only transition observed with variation

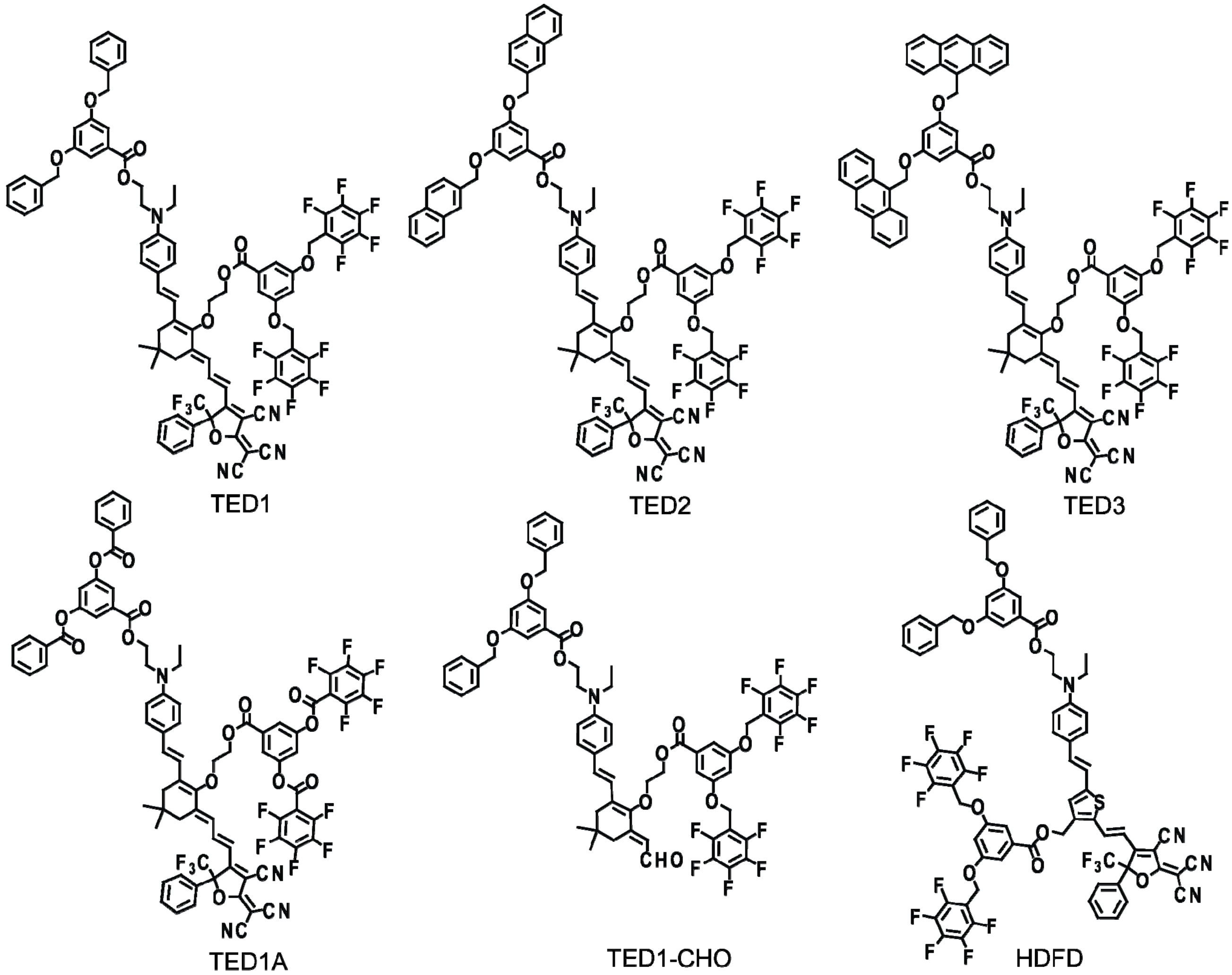
TED1
TED2
TED3
TED1A
TED1-CHO
HDFD

Figure 2. Structures of HDFD and related (TED) chromophore-containing dendrimers.

of temperature is the glass transition temperature (T_g). This behavior is well-known for polymer materials and is also detected reliably by differential scanning calorimetry (DSC) measurements. When MAP interactions are present, an additional transition (denoted as T_l) is observed below the glass transition temperature. If SM-FM, IFA, and DRS data are combined, an activation entropy (ΔS^*) and correlation length or dissipation length for cooperative motion (ξ) can be estimated. For the C1 dendritic chromophore-containing material of Fig. 1, $|T\Delta S^*| \approx 56$ kcal and $\xi \approx 55$ nm (at 106°C—a temperature above T_g). Determination of the correlation (or dissipation) length requires that the temperature regions of IFA and DRS data overlap thus the range over which ξ can be determined is limited. ξ decreases with increasing temperature above T_g so ξ can be expected to be greater than 55 nm at T_g. Optimum poling efficiency occurs at the temperature where the largest ΔS^* is observed (see Fig. 4 for data obtained for the C1 material).[39] When order parameter data and viscoelastic data are correlated, a self-consistent picture of the impact of MAP interactions emerges.

MAP effects are also important in optimizing the optical nonlinearity/optical loss ratio. Increasing $\langle\cos^3\theta\rangle$ permits r_{33} to be increased without any deleterious effect on optical loss while it is, in general, difficult to increase molecular first hyperpolarizability (β) or chromophore number density (N) without also increasing absorption loss (although this observation does not hold for all chromophores). Another important characteristic of OEO materials important for optimized device performance is stability (both thermal and photochemical stability) under operational conditions. Thermal and photostability are usually related to the material glass transition temperature (lattice hardness).

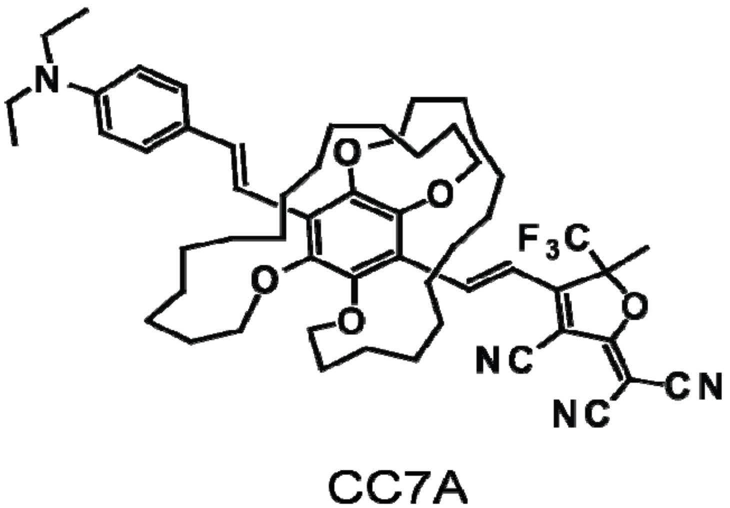

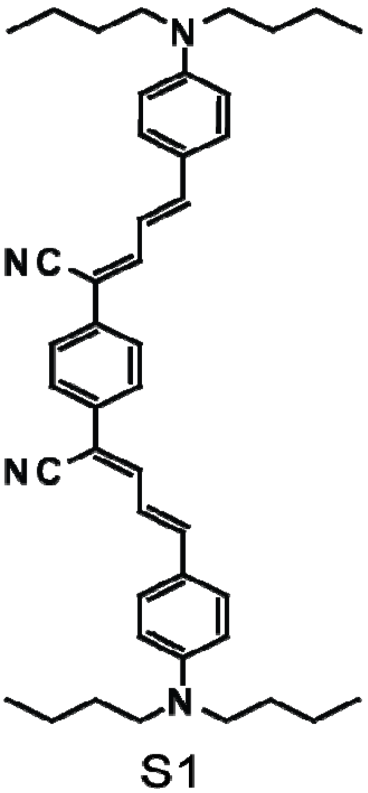

Figure 3. Structures of non-dendrimer chromophores are shown.

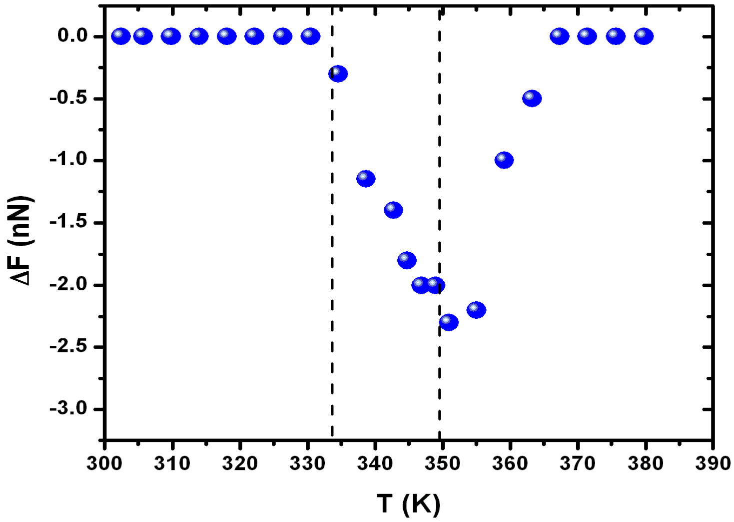

Figure 4. The temperature dependence of activation entropy is shown (ΔF is proportional to TΔS*/ϕ where ΔS* is the activation entropy and ϕ is stress activation volume). ΔF is determined from intrinsic friction analysis (IFA).[36] The optimum poling temperature for C1 occurs at T ≈ 350K. A nonzero ΔF value is indicative of cooperative molecular motion (an entropic contribution) while a zero value of ΔF indicates that only an enthalpic contribution is present. Figure from reference 39.

Stability is commonly improved as the result of MAP interactions. Also, some MAP moieties (e.g., coumarins) are capable of being photo-crosslinked further elevating the glass transition temperature. While the discussion thus far has focused on OEO materials prepared by electric field poling, the same considerations with respect to intermolecular electrostatic interactions (including MAP interactions) also apply to materials prepared by crystal growth and sequential synthesis/self-assembly.

It should be clear that optimizing material electro-optic activity is challenging and requires a detailed understanding of the role played by various intermolecular electrostatic interactions. Statistical mechanical calculations have been of substantial utility in guiding the design of new materials through simulation of the effects of various specific interactions. A further challenge in material design and processing arises in integrating OEO materials into various types of devices. A major challenge with device structures is that of achieving the same "effective" local (at the chromophore) poling field in a device configuration that is achieved for poling a single thin film. Indeed, poling fields in devices can be attenuated by factors of 2-10 with a resulting reduction in macroscopic electro-optic activity. This attenuation can be associated with two factors: (1) the conductivity of the OEO material relative to other materials[40] and (2) increased separation of poling electrodes. A critical issue with silicon photonic, metamaterial, and plasmonic device structures is that of controlling optical loss. With silicon photonics, the high index of refraction of silicon permits waveguide dimensions to be reduced to 400-500 nm. Light can be further concentrated to sub-λ dimensions by cutting 25-150 nm slots into the silicon waveguides. These slots can be filled with OEO materials; and when doped silicon is employed as poling and drive electrodes, drive voltages (V_π) at 1550 nm of less than 1 volt have been achieved (although the effective EO activity is only on the order of 30 pm/V).[8,11] Such slotted waveguide structures are referred to as vertical slot structures and optical loss observed for such devices is very sensitive to wall roughness and hence to mask resolution. Another variant of the vertical structure is a nanowire structure recently described by Norwood and Peyghambarian.[12] Horizontal slot structures have also been fabricated and explored.[41] These have the advantage of providing a planar deposition surface for the OEO material and they also permit corona poling to be pursued. Horizontal slot structures are also the logical choice for utilization of crystalline materials and materials prepared by sequential synthesis/self-assembly.[34] Slotted silicon photonic waveguides have also been integrated with photonic crystal (bandgap) device structures to further decrease voltage-length products and products as low as 0.56 V-mm (effective r_{33} of 132 pm/V) have been achieved although at the price of bandwidth limitation.[35] Plasmonic devices involve the integration of metal with EO materials although most reported studies to the present deal with integration of inorganic liquid crystalline materials or exploitation of metal/oxide/silicon field effect modulation[42] rather than OEO materials[14]. A significant problem with both plasmonic and metamaterial devices is optical loss. Fortunately, the loss problem is somewhat ameliorated by shorter device lengths, which is also important for electronic/photonic integration particularly chipscale integration. Integration of OEO materials is very important for electronic/photonic integration due to the potential for reduction of thermal management problems facilitated by the large electro-optic activity of OEO materials.

2. RECENT RESULTS

This communication provides an update to references 14 and 39, reporting recently expanded studies of optimization of electro-optic activity and the integration of OEO materials into device structures. The preceding section has provided an introduction to selected proof-of-concept examples while we now turn our attention to expanded studies including the investigation of additional material systems (Figs. 1-3) and a variety of different nanostructured metal plasmonic device structures. The present communication concentrates on the conclusions derived from expanded studies. The details of methods and analysis are deferred other publications where they can be discussed in-depth. For example, viscoelastic effects for the materials of Figs. 1-3 have been investigated by SM-FM, IFA, DRS, and molecular dynamical calculations utilizing different force fields.[37] The details of these studies, and other results discussed here, are beyond the scope of this communication but can be found elsewhere.[37,38]

2.1 Systematic Optimization of Electro-Optic Activity

The objective of our recent studies is to define the various contributions made by chromophore dipolar, dendron (arene/perfluoroarene and coumarin), and van der Waals interactions to chromophore acentric order. We have expanded our earlier studies of C1 and FTC/PMMA (Table 1) to the materials of Table 2 (see Figs 1-3 for structures of materials).

Table 2. Transition temperatures determined from SM-FM (T_l and T_g) and DSC (T_g) measurements.

Material	T_l (°C)	T_g (°C)	$T_g - T_l$ (°C)	DSC T_g (°C)
S1	--	36±1	--	
TED1-CHO	41±2	46±2	5	50
C1-CHO	42±2	47±2	5	
CE	50±3	59±2	9	
CC7	--	60±2	--	
HDFD	59±2	70±2	10	70
TED1	59±2	74±2	15	80
C1	61±2	76±2	15	80
TED2	75±2	86±2	11	92
TED1A	80±2	93±3	13	106
TED3	118±2	126±2	8	125

The structures are varied to achieve materials with and without dipolar interactions or with reduced dipolar interactions, with and without dendron interactions (coumarins and arene/perfluoroarene substituents), and as a function of size/molecular weight of substituents. In addition to investigating the materials of Table 2 as neat materials, the CC7 chromophore was studied as composite materials prepared by dissolving the chromophore in amorphous polycarbonate (APC). As with chromophore/polymer (PMMA and APC) composite materials previously studied,[37,39] materials (S1 and CC7) that do not contain dendritic moieties do not exhibit the T_l transition. The presence of the T_l transition and finite ΔF values (from IFA) for dendron-containing materials indicate the presence of cooperative molecular motion responsible for reduced lattice dimensionality. From the above table and IFA analysis, it is clear that both chromophore dipolar interactions and dendron (arene/perfluoroarene and coumarin) interactions contribute to cooperative motion and to ΔS^*. C1-CHO and TED1-CHO (compared to C1 and TED1) illustrate the effect that systematically reducing chromophore dipolar interactions has upon cooperativity. It is also interesting to compare data for C1 and its cinnamic ester analog, CE. The coumarin moiety is well-known for its liquid crystal forming property while the cinnamic ester analog does not exhibit such LC phase formation. The EO chromophore is the same in both C1 and CE so the difference in behavior largely reflects the role played by the coumarin moiety in influencing molecular cooperativity. The behavior of ΔF with temperature for C1, C1-CHO, and CE is qualitatively illustrated in Fig. 3; that is, ΔF increases as the glass transition temperature is approached and then decreases (ultimately to zero). As already noted, determination of the correlation (or dissipation) length, $\xi(= \nu_p/f_p)$ requires temperature regions where the peak velocity (ν_p) from SM-FM/IFA and the peak relaxation frequency (f_p) from DRS overlap. As already noted, such temperatures are currently above the glass transition temperatures of the materials (e.g., a value of $\xi = 55$ nm for C1 at 106°C compared to a T_g of 80°C for C1 and a value of $\xi = 15$ nm for TED3 at 158°C compared to a T_g of 125°C). Thus, it is impossible at this point in time to define correlation lengths at the optimum poling temperatures but it is clear that at such temperatures the correlation lengths are at least on the order of many tens of nanometers. It is also important to note a subtle difference in the behavior of the C1 and HDFD/TED materials. While |ΔF| goes through a maximum for the C1 materials, it continues to increase above T_g for the HDFD/TED materials. Since ΔF also depends on the stress activation volume, ϕ, and since we do not know the temperature dependence of ϕ, it is impossible to know how ΔS* is changing with temperature.

Molecular dynamic simulations and conformational calculations[37] have been carried out to understand various contributions to activation energies associated with cooperative effects. The discussion of these simulations are beyond the scope of this communication but they do support the conclusion derived from analysis of SM-FM, IFA, and DRS results that chromophore dipolar and dendron interactions make a dominant contribution to cooperativity. For the materials of Table 2, about 70-80% of the measured (by SM-FM and IFA) activation energies can be attributed to cooperativity (entropic effects) leading to TΔS* values of many tens of kilocalories at the optimum poling temperature. The contributions of various dendron intermolecular electrostatic interactions (coumarin-coumarin and arene-perfluoroarene) to activation energies are approximately 1.5 to 2.5 times greater than the contribution from full chromophore-chromophore dipolar interactions.

Recent studies illustrate the importance of a judicious choice of specific spatially-anisotropic interactions to enhance poling-induced acentric order. If interactions (e.g., such as hydrogen bonding) are too strong, the ability of chromophores to reorient under poling conditions is lost and microdomain formation becomes a serious problem (particularly in terms of increased optical loss). Thus, our next steps are judiciously cautious and we are in the process of synthesizing the following compound in which the heteroaromatic bridge of C1 is replaced with an isophorone-protected polyene bridge.

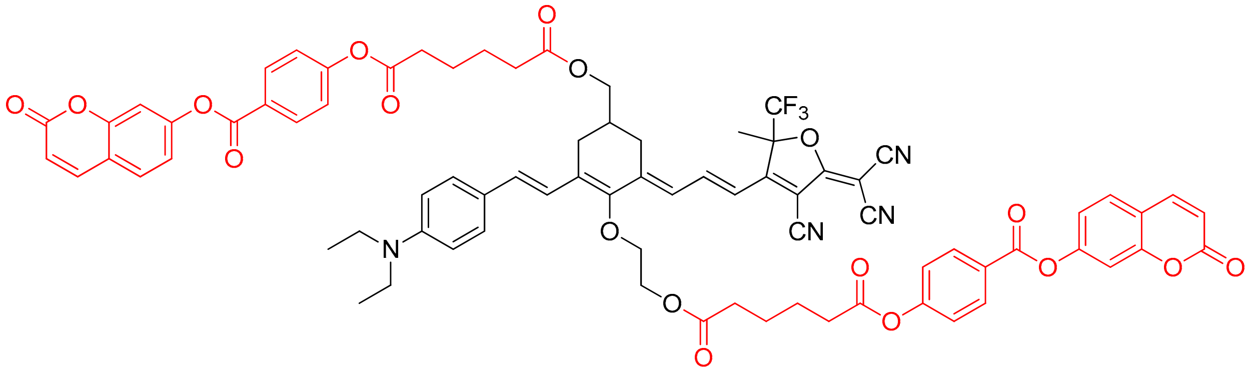

Figure 5. The structure of a new EO material currently being synthesized is shown. Variants, where the coumarin moieties are attached to the ends of the chromophore, are also being prepared.

The improved molecular hyperpolarizability of the chromophore of this material should by itself lead to a substantial increase in electro-optic activity. There is also the potential for improved acentric order due to the effect of coumarin interactions (for this new geometry) on lattice dimensionality.

2.2 Integration of OEO Materials

In previous work, we have demonstrated the integration of OEO materials into vertical and horizontal slot silicon photonic device structures and into plasmonic and metamaterial structures. Because of space limitations here, we limit discussion to plasmonic EO devices. We have investigated IMI (insultator-metal-insulator) and MIM (metal-insulator-metal) plasmonic devices based on continuous and discontinuous (nanostructured) gold and silver. The behavior of continuous metal films is dominated by long-range surface plasmon polaritons (LRSPPs).[43] The optical loss of devices based on these films is so high as to not warrant further discussion here. With discontinuous (nanostructured) metal films, performance can be dominated either by LRSPPs or by long-range surface modes (LRSMs). The transition from LRSM to LRSPP behavior is shown in Fig. 6 for discontinuous gold films. The difference in dielectric properties of continuous and discontinuous films accounts for the difference in optical properties. For discontinuous films, $\varepsilon_m = -4.9 + i8.8$ (for p-polarized light at 633 nm and $\varepsilon_m = -3.0 + 8.7$ (for s-polarized light at 633 nm). For continuous films, ε_m = -

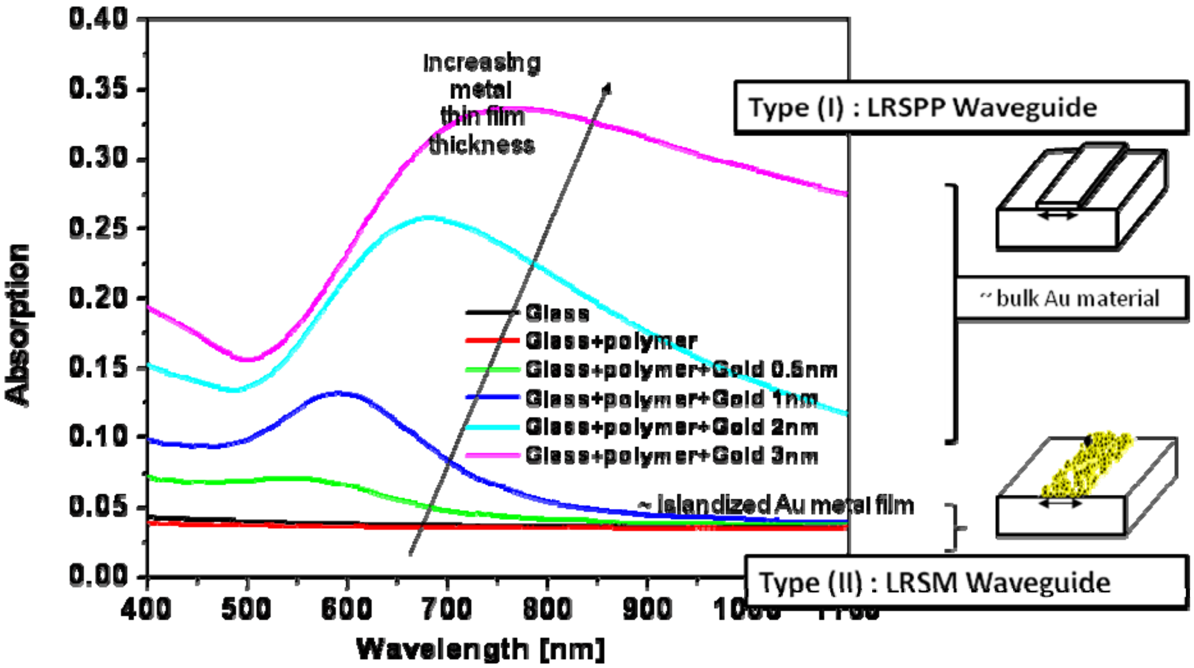

Figure 6. Absorption of spectra as a function of discontinuous gold film thickness and illustration of the transition from LRSM to LRSPP behavior.

131.95 + i12.55 (1550 nm; only TM mode supported). The advantage of utilizing LRSMs is reduced optical loss and the fact that both TM and TE modes are supported. Also, the LRSM modes are more spherical than LRSPP modes. We have explored the use of discontinuous films for the fabrication of both amplitude (push-pull Mach Zehnder) and phase modulators. A variety of OEO materials have been explored but we limit the present discussion to the utilization of the DH6-APC (see Fig. 7) and AJ309/AJ416 materials. The characteristics of the DH6-APC material and the Mach Zehnder modulator fabricated using it are given in Fig. 7. The upper and lower cladding materials are the commercially-available polymers UFC-170A and UV-15. The islandized gold metal thickness is 1 nm (10 angstroms) and the interaction length is 1 cm. The measured V_π is 17.8 V (for single arm driving—push-pull operation reduces the drive voltage by 50%). The insertion loss is 14 dB (fiber-to-waveguide-to-lens). The propagation loss at 1550 nm is 0.65-0.7 dB/mm (see Fig. 8). We have also fabricated this plasmonic Mach Zehnder modulators with the AJ309/AJ416 materials. With more active materials and a 1.5 cm device length, the drive voltage (V_π) is reduced to 3.94 V (single arm drive). We have used the AJ309/AJ416 OEO materials with a phase modulator device structure (2 nm islandized gold and 8 mm interaction length). The V_π voltage is 5.39 V. We have also fabricated MIM plasmonic phase modulators (device length of 1.5 cm, and waveguide gap of 4 microns. The fiber-to-lens optical loss was determined to be 16-19 dB. For comparison a plasmonic LRSPP MIM phase modulator (TM mode; 2.5 mm interaction length, metal film gap of 4 micron) displays a drive voltage of > 30 V and an insertion loss of > 25 dB. We have also demonstrated that plasmonic device structures can be used to focus light to nanoscopic dimensions. One of the device structures being investigated is shown in Fig. 9.

3. CONCLUSIONS

Exploitation of coumarin and arene/perfluorarene interactions permit acentric order to be increased to 0.15 associated with the reduction of lattice dimensionality from 3-D or 2-D. Materials under development should permit electro-optic activity to be increased to values approaching 500 pm/V. Intermolecular interactions that enhance acentric order also facilitate the minimization of optical loss and are relevant to improving the performance of all classes of OEO materials (electrically-poled thin films, thin films prepared by sequential synthesis/self assembly, and crystalline thin films). The coumarin moiety also facilitates post-poling elevation of the material glass transition temperature by crosslinking..

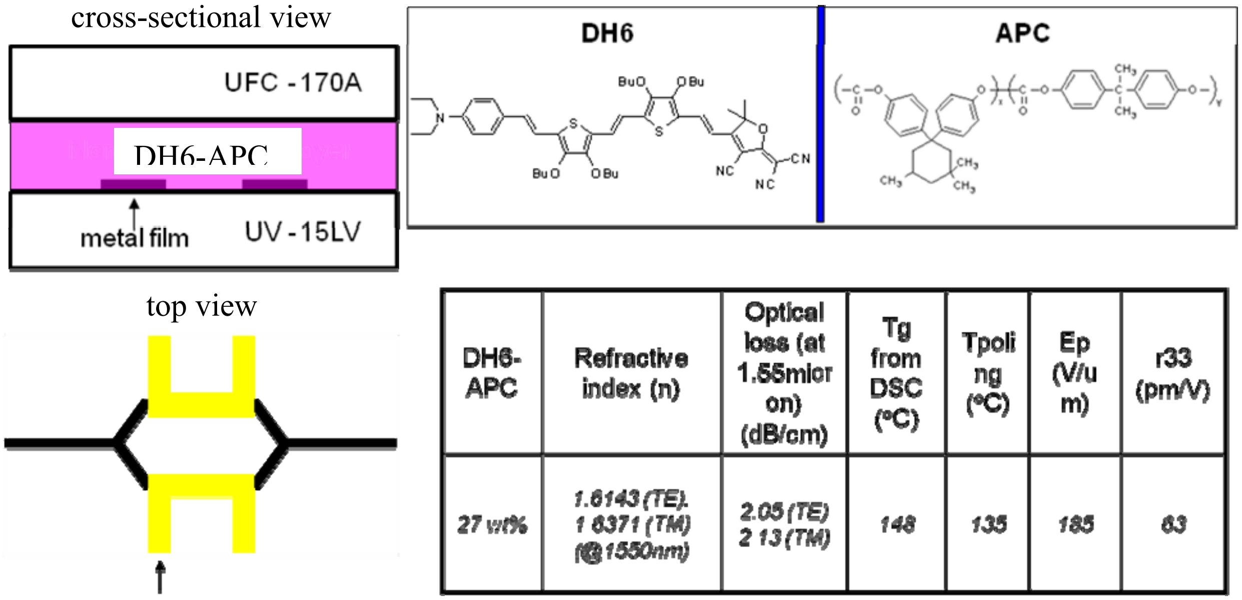

DH6-APC	Refractive index (n)	Optical loss (at 1.55micron) (dB/cm)	Tg from DSC (°C)	Tpoling (°C)	Ep (V/um)	r33 (pm/V)
27 wt%	*1.6143 (TE). 1 6371 (TM) (@1550nm)*	*2.05 (TE) 2 13 (TM)*	*148*	*135*	*185*	*63*

Fig. 7. Cross-sectional and top views of the push-pull Mach Zehnder amplitude modulator employing discontinuous (nanostructured) metal films are shown as is the structure of the DH6 chromophore and the host APC polymer. Also shown are the characteristics of the DH6-APC composite and the poling condition.

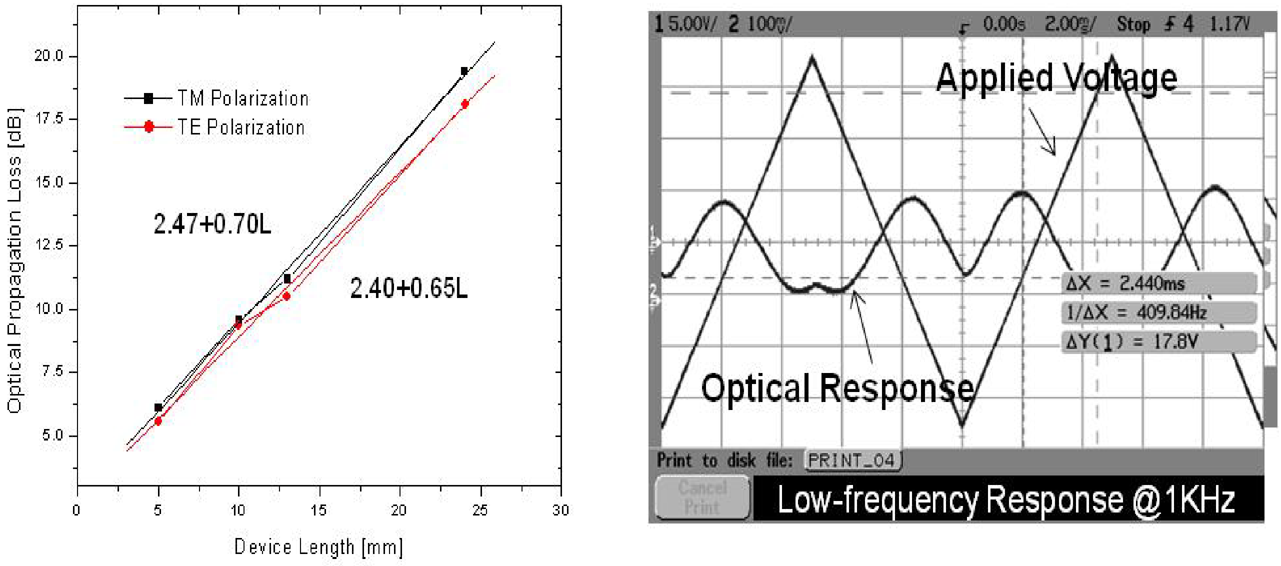

Figure 8. The optical loss (left) and electro-optic response (right) are shown for an IMI plasmonic structure prepared using the DH6-APC OEO material.

Control of lattice dimensionality appears to be an effective paradigm for optimization of OEO performance for currently-available chromophores. It is not yet clear that lattice dimensionality can be decreased below 2-D and it has been difficult to develop new classes of chromophores with improved molecular hyperpolarizability. Baring advances in these two areas, the current paradigm may define the state-of-the-art of OEO materials for some time. Work to the present has illustrated the importance of considering the effects of chromophore dipolar interactions, specific dendron intermolecular interactions, covalent bond potentials, nuclear steric effects, and van der Waals interactions in controlling poling-induced acentric order.

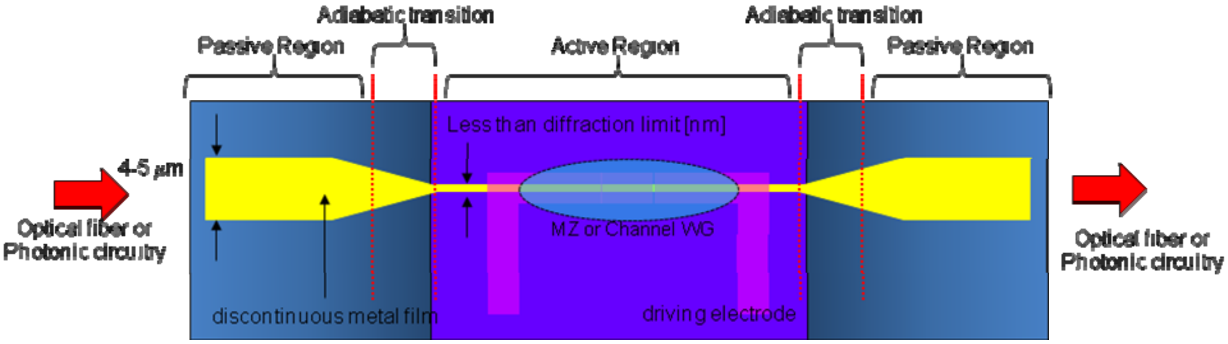

Figure 9. An EO modulator effecting sub-wavelength (λ) concentration of light

Exploration of new device structures for silicon photonic, plasmonic, and metamaterial devices is an active research direction and is likely to lead to significant further improvements in device performance including effective EO activity and insertion loss. Optimization of device bandwidth and exploitation of reduced device dimensions are also important research objectives. The LRSM plasmonic device structures discussed in the preceding paragraphs demonstrate a significant reduction in optical loss while facilitating reduction in device dimensions and sub-wavelength concentration of light. The potential for sub-1 centimeter device lengths, sub-1 volt drive voltages, and insertion loss values less than 5 dB that can be realized by the use of optimized OEO materials together with novel device designs is extremely important for electronic/photonic integration and particularly for chipscale integration. To the present time, the best results have been obtained for slotted silicon photonic waveguide and nanowire devices. However, the present study also illustrates the potential for plasmonic devices.

ACKNOWLEDGMENTS

The authors gratefully acknowledge partial financial support for this research from the National Science Foundation (DMR-0905686 and DMR-0120967) and the Air Force Office of Scientific Research (FA9550-09-1-0589 and FA9550-09-1-0682). The authors also thank Michael Hochberg, Antao Chen, B. E. Eichinger, J. Park, P. Berini, K. Geary, W. Steier and members of the Jen and Dalton Research Groups for contributing to this research and for many helpful discussions. We thank Lumera Corporation for providing samples of the DH6 chromophore.

REFERENCES

[1] Chen, D., Fetterman, H. R., Chen, A., Steier, W. H., Dalton, L. R., Wang, W. and Shi, Y., "Demonstration of 110 GHz Electro-Optic Polymer Modulators," Appl. Phys. Lett. 79, 3335-3337 (1997).

[2] Lee, M., Katz, H. E., Erben, C., Gill, D. M., Gopalan, P., Heber, J. D. and McGee, D. J. "Ultra-Fast Modulation of Light Using an Electro-Optic Polymer," Science 289, 1404-1407 (2002).

[3] Drenser, K. A., Larsen, R. J., Strohkendl, F. P. and Dalton L. R., "Femtosecond Frequency-Agile, Phase-Sensitive-Detected, Multi-Wave-Mixing Nonlinear Optical Spectroscopy Applied to π-Electron Photonic Materials," J. Phys. Chem. 103, 2290-2301 (1999).

[4] McLaughlin, C. V., Hayden, L. M., Polishak, B., Huang, S. M., Luo, J. M., Kim, T. M., Jen. A. K. "Wideband 15 THz Response Using Organic Electro-Optic Polymer Emitter-Sensor Pairs at Telecommunications Wavelengths," Appl. Phys. Lett. 92 (15), 151107-1-3 (2008).

[5] Hochberg, M., Baehr-Jones, T., Wang, G., Shearn, M., Harvard, K., Liu, J., Chen, B., Shi, Z., Lawson, R., Sullivan, P. A., Jen, A. K.-Y., Dalton, L. R., and Scherer, A. "All Optical Modulator in Silicon with Terahertz Bandwidth," Nature Mater. 5, 703-709 (2005).

[6] Baehr-Jones, T., Hochberg, M., Wang, G., Lawson, R., Liao, Y., Sullivan, P. A., and Dalton, L. R., "Optical Modulation and Detection in Slotted Silicon Waveguides," Opt. Exp. 13, 5216-5226 (2005).

[7] Hochberg, M., Baehr-Jones, T., Wang, G., Huang, J., Sullivan, P. A., Dalton, L. R., and Scherer, A., "Toward a millivolts optical modulator with nano-slot waveguides," Opt. Exp. 15, 8401-8410 (2007).

[8] Baehr-Jones, T., Penkov, B., Huang, J., Sullivan, P. A., Davies, J., Takayesu, J., Luo, J., Kim, T.-D., Dalton, L. R., Jen, A. K.-Y., and Hochberg, M., "Nonlinear Polymer-Clad Silicon Slot Waveguide Modulator With a Half Wave Voltage of 0.25 V," Appl. Phys. Lett. 92, 163303-1-3 (2008).

[9] Takayesu, J., Hochberg, M., Baehr-Jones, T., Chan, E., Wang, G., Sullivan, P. A., Liao, Y., Davies, J., Dalton, L. R., Scherer, A., and Krug, W., "A Hybrid Electro-Optic Microring Resonator-Based 1x4x1 ROADM for Wafer Scale Optical Interconnects," IEEE J. Lightwave Technol. 27 (4), 440-448 (2008).

[10] Wulbern, J. H., Hampe, J., Petrov, A., Eich, M., Luo, J., Jen, A. K.-Y., Falco, A. D., Krauss, F., and Bruns, J., "Electro-Optic Modulation in Slotted Resonant Photonic Crystal Heterostructures," Appl. Phys. Lett. 94 (24), 241107-1-3 (2008).

[11] Ding, R., Baehr-Jones, T., Liu, Y., Bojko, R., Witzens, J., Huang, S., Luo, J., Benight, S., Sullivan, P., Fedeli, J.-M., Fournier, M., Dalton, L. R., Jen, A. K.-Y., and Hochberg, M., "Demonstration of a Low $V_{\pi}L$ Modulator With GHz Bandwidth Based on Electro-Optic Polymer-Clad Silicon Slot Waveguides," Opt. Exp. 18 (15), 15618-15623 (2010).

[12] Norwood, R., private communication.

[13] Lin, C.-Y., Wang, X., Chakravarty, S., Lee, B. S., Lai, W., Luo, J., Jen, A. K.-Y., and Chen, R. T. "Electro-Optic Polymer Infiltrated Silicon Photonic Crystal Slot Waveguide Modulator With 23 dB Slow Light Enhancement," Appl. Phys. Lett. 97, 093304-1-3 (2010).

[14] Kim, S.-K., Sylvain, N., Benight, S. J., Kosilkin, I., Bale, D. H., Robinson, B. H., Geary, K., Jen, A. K.-Y., Steier, W. H., Fetterman, H. R., Berini, P. and Dalton, L. R., "Active Plasmonic and Metamaterials and Devices," Proc SPIE 7754, 775403 1-10 (2010).

[15] Dalton, L. R., Robinson, B. H., Jen, A. K.-Y., Steier, W. H., and Nielsen, R., "Systematic Development of High Bandwidth, Low Drive Voltage Electro-Optic Devices and Their Applications," Opt. Mater. 21, 19-28 (2003).

[16] Nielsen, R. D. and Robinson, B. H., "Simulation of the Loading Parameter in Organic Nonlinear Optical Materials," J. Phys. Chem. B 108, 8659-8667 (2004).

[17] Shi, Y., Zhang, C., Zhang, H., Bechtel, J. H., Dalton, L. R., and Robinson, B. H., "Low (Sub-1Volt) Halfwave Voltage Polymeric Electrooptic Modulators Achieved by Control of Chromophore Shape," Science 288, 119-122 (2000).

[18] Sullivan, P. A., Rommel, H., Liao, Y., Olbricht, B. C., Akelaitis, A. J. P., Firestone, K. A., Kang, J.-W., Luo, J., Choi, D. H., Eichinger, B. E., Reid, P. J., Chen, A., Jen, A. K.-Y., Robinson, B. H. and Dalton, L. R., "Theory Guided Design and Synthesis of Multi-Chromophore Dendrimers: An Analysis of the Electro-Optic Effect," J. Amer. Chem. Soc. 129, 7523-7530 (2007).

[19] Sullivan, P. A., Rommel, H. L., Takimoto, Y., Hammond, S. R., Bale, D. H., Olbricht, B. C., Liao, Y., Rehr, J., Eichinger, B. E., Jen, A. K.-Y., Reid, P. J., Dalton, L. R. and Robinson, B. H., "Modeling the Optical Behavior of Complex Organic Media: From Molecules to Materials," J. Phys. Chem. B 113 (47), 15581-15588 (2009).

[20] Dalton, L. R., Sullivan, P. A. and Bale, D. H., "Electric Field poled Organic Electro-Optic Materials: State of the Art and Future Prospects," Chem. Rev. 110, 25-55 (2010).

[21] Sullivan, P. A. and Dalton, L. R., "Theory-Inspired Development of Organic Electro-Optic Materials," Acc. Chem. Res. 43 (1), 10-18 (2010).

[22] Zhou, Z. Luo, J. Huang, S., Kim, T.-D., Shi, Z., Cheng, Y., Jang, S., Knorr, D. B. Jr., Overney, R. M. and Jen, A. K.-Y., "Supramolecular self-assembled dendritic nonlinear optical chromophores: Fine-tuning of arene-perfluoroarene interactions for ultralarge electro-optic activity and enhanced thermal stability," Adv. Mater. 21 (19), 1976-1981 (2009).

[23] Benight, S. J., Bale, D. H., Olbricht, B. C. and Dalton, L. R. "Organic Electro-Optics: Understanding Material Structure/Function Relationships and Device Fabrication Issues," J. Mater. Chem. 19, 7466-7475 (2009).

[24] Benight, S. J., Johnson, L. E., Barnes, R., Olbricht, B. C., Bale, D. H., Eichinger, B. E., Dalton, L. R., Sullivan, P. A., and Robinson, B. H., "Reduced dimensionality in organic electro-optic materials," J. Phys. Chem. B 114 (37), 11949-11956 (2010).

[25] Benight, S. J., Johnson, L. E., Krorr, D. B. Jr., Elangovan, A., Kosilkin, I., Olbricht, B. C., Sullivan, P. A., Bale, D. H., Robinson, B. H., Overney, R. M., Jen, A. K.-Y., Steier, W. H., Kim, S.-K., Fetterman, H. R., Prather, D. W. and Dalton, L. R., "Theory-Guided Enhancement of Poling Efficiency of Organic Electro-Optic Materials," Proc. SPIE 7774, 77740F 1-12 (2010).

[26] Dalton, L. R., Benight, S. B., Johnson, L. E., Knorr, D. B. Jr., Kosilkin, I., Eichinger, B. E., Robinson, B. H., Jen, A. and Overney, R., "Systematic Nano-Engineering of Soft Matter Organic Electro-Optic Materials," Chem. Mater. 23, ASAP article (2010).

[27] Kin, T-D., Lao, J., Cheng, Y.-J., Shi, Z., Hau, S., Jang, S.-H., Zhou, X.-H., Tian, Y., Polishak, B., Huang, S., Ma, H., Dalton, L. R., and Jen, A. K.-Y., "Binary Chromophore Systems in Nonlinear Optical Dendrimers and Polymers for Large Electro-Optic Activities," J. Phys. Chem. C 112 (21), 8091-8098 (2008).

[28] Dalton, L. R., Sullivan, P. A., Bale, D. H., Olbricht, B. C., Davies, J. A., Benight, S. J., Kosilkin, I., Robinson, B. H., Eichinger, B. E., and Jen, A. K. Y., "Organic electro-optic materials: Understanding structure/function relationships critical to the optimization of electro-optic activity," in [Organic Thin Films for Photonics Applications] eds. Herman, W. and Foulger, S., Amer. Chem. Soc., Washington, DC, 13-33 (2010).

[29] Zhou, X.-H., Luo, J., Kim, T.-D., Jang, S.-H., Overney, R. M., Dalton, L. R., and Jen, A. K.-Y., "Molecular design and supramolecular organization of highly efficient nonlinear optical chromophores for exceptional electro-optic properties," in [Organic Thin Films for Photonics Applications] eds. Herman, W. and Foulger, S., Amer. Chem. Soc., Washington, DC, 51-56 (2010).

[30] Olbricht, B. C., Sullivan, P. A., Wen, G.-A., Mistry, A., Davies, J. A., Ewy, T. R., Eichinger, B. E., Robinson, B. H., Reid, P. J., and Dalton, L. R., "Laser-assisted poling of binary chromophore materials," J. Phys. Chem. C 112 (21), 7983-7988 (2008).

[31] Robinson, B. H. and Dalton, L. R., "Monte Carlo Statistical Mechanical Simulations of the Competition of Intermolecular Electrostatic and Poling Field Interactions in Defining Macroscopic Electro-Optic Activity for Organic Chromophore/Polymer Materials. J. Phys. Chem. A 104 (20), 4785-4795 (2000).

[32] Olbricht, B. C.; Sullivan, P. A.; Davies, J. A.; Dennis, P. C.; Hurst, J. T.; Johnson, L. E.; Bale, D. H.; Benight, S. J.; Hilfiker, J. N.; Chen, A.; Eichinger, B. E.; Reid, P. J.; Dalton, L. R.; Robinson, B. H. Measuring order in contact-poled organic electro-optic materials with variable angle polarization-referenced absorption spectroscopy (VAPRAS)," J. Phys. Chem. B, ASAP article (2010).

[33] Gray, T., Kim, T.-D., Knorr, D. B. Jr., Luo, J., Jen, A. K.-Y. and Overney, R. M., "Mesoscale Dynamics and Cooperativity of Networking Dendronized Nonlinear Optical Molecular Glasses," Nano Lett. 8 (2), 754-759 (2008).

[34] Knorr, D. B. Jr., Zhou, X-H., Shi, Z.; Luo, J., Jang, S.-H., Jen, A. K.-Y. and Overney, R. M., "Molecular Mobility in Self-Assembled Dendritic Chromophore Glasses," J. Phys. Chem. B 113 (43), 14180-14188 (2009).

[35] Gray, T., Kilgore, J. P., Luo, J., Jen, A. K.-Y. and Overney, R. M., "Molecular Mobility and Transitions in Complex Organic Systems Studied by Shear Force Microscopy," Nanotechnology 18 044009-1-9 (2007).

[36] Knorr, D. B. Jr., Gray, T. O. and Overney, R. M, "Intrinsic Friction Analysis—Novel Nanoscopic Access to Molecular Mobility in Constrained Organic Systems," Ultramicroscopy 109 (8), 991-1000 (2009).

[37] Knorr, D. B. Jr., "Molecular Relaxations in Constrained Nanoscale Systems," Ph.D. Thesis, University of Washington, Seattle (2010), see particularly Chapter 6: "Internal Constraints: Non-Linear Optical Materials". Publication of methods and results is in preparation.

[38] Benight, S. J. and Knorr, D. B. Jr., unpublished data to be published.

[39] Benight, S. J., Johnson, L. E., Knorr, D. B. Jr., Elangovan, A., Kosilkin, I., Olbricht, B. C., Sullivan, P. A., Bale, D. H., Robinson, B. H., Overney, R. M., Jen, A. K.-Y., Steier, W. H., Kim, S.-K., Fetterman, H. R., Prather, D. W. and Dalton, L. R., "Theory-Guided Enhancement of Poling Efficiency of Organic Electro-Optic Materials," Proc. SPIE 7774, 77740F 1-12 (2010).

[40] Huang, S., Kim, T.-D., Luo, J., Hau, S. K., Shi, Z., Zhou, X.-H., Yip, H.-Y. and Jen, A. K.-Y, "Highly Efficient Electro-Optic Polymers Through Improved Poling Using a Thin TiO_2-modified Transparent Electrode," Appl. Phys. Lett. 96, 243311-1-3 (2010).

[41] Figi, H., Bale, D. H., Szep, A., Dalton, L. R. and Chen, A., "Electro-Optic Modulation in Horizontally Slotted Silicon/Organic Crystal Hybrid Devices," J. Opt. Soc. Amer. submitted.

[42] Dionne, J. A., Kiest, K., Swetlock, L. A. and Atwater, H. A., "PlasMOStor: A Metal/Oxide/Si Field Effect Plasmonic Modulator," Nano Lett. 9(2), 897-902 (2009).

[43] Berini, P., "Long-Range Surface Plasmon Polaritons," Advances in Optics and Photonics 1, 481-588 (2009).